CONTRACT REPORT ARBRL-CR-00473

DIAGNOSTICS OF GUN BARREL PROPELLANTS

Prepared by

Polytechnic Institute of New York
Route 110
Farmingdale, New York 11735

November 1981

US ARMY ARMAMENT RESEARCH AND DEVELOPMENT COMMAND
BALLISTIC RESEARCH LABORATORY
ABERDEEN PROVING GROUND, MARYLAND

REPORT DOCUMENTATION PAGE

READ INSTRUCTIONS BEFORE COMPLETING FORM

1. REPORT NUMBER: CONTRACT REPORT ARBRL-CR-00473	2. GOVT ACCESSION NO.
3. RECIPIENT'S CATALOG NUMBER	
4. TITLE (and Subtitle): Diagnostics of Gun Barrel Propellants	5. TYPE OF REPORT & PERIOD COVERED: Scientific Final
6. PERFORMING ORG. REPORT NUMBER	
7. AUTHOR(s): S. Lederman, R. Cresci, T. Posillico	8. CONTRACT OR GRANT NUMBER(s): DAAK11-79-C-0128
9. PERFORMING ORGANIZATION NAME AND ADDRESS: Polytechnic Institute of New York, Route 110, Farmingdale, New York 11735	10. PROGRAM ELEMENT, PROJECT, TASK AREA & WORK UNIT NUMBERS
11. CONTROLLING OFFICE NAME AND ADDRESS: US Army Armament Research & Development Command, US Army Ballistic Research Laboratory (DRDAR-BL), Aberdeen Proving Ground, MD 21005	12. REPORT DATE: November 1981
	13. NUMBER OF PAGES: 43
14. MONITORING AGENCY NAME & ADDRESS(if different from Controlling Office)	15. SECURITY CLASS. (of this report): Unclassified
	15a. DECLASSIFICATION/DOWNGRADING SCHEDULE

16. DISTRIBUTION STATEMENT (of this Report)

Approved for public release; distribution unlimited

17. DISTRIBUTION STATEMENT (of the abstract entered in Block 20, if different from Report)

N/A

18. SUPPLEMENTARY NOTES

19. KEY WORDS (Continue on reverse side if neceesary and identify by block number)

laser
Spontaneous Raman
temperature
propellant
projectile

20. ABSTRACT (Continue on reverse side if neceseary and identify by block number)

A preliminary investigation on the applicability of the spontaneous Raman diagnostic technique to the determination of the temperature of the propellant gases in the vicinity of the muzzle of a 20mm gun has been completed. It was concluded that with the proper care, and the correct laser excitation wavelength, flow field diagnostics based on laser light scattering can provide most of the information desired. In partic-

20. Abstract - Continued

ular, the spontaneous Raman technique can successfully be utilized in the solution of this problem.

TABLE OF CONTENTS

LIST OF ILLUSTRATIONS

Diagnostics of Gun Barrel Propellants

I. Introduction

Several problems exist in the use of high performance cannon which require a detailed knowledge of the thermodynamic properties of the propellant gases both within the gun barrel and after they leave the muzzle. One of these is the barrel erosion which occurs in tank guns when high performance ammunition is fired. In order to better understand, and subsequently eliminate this problem the heat transfer to the surface must be determined; this is directly related to the gas composition and thermodynamic properties within the barrel. Muzzle flash is another serious problem with all guns but is particularly important in artillery because of increased vulnerability to detection and reduced night vision of the operators. Any attempt to accurately model muzzle flash depends on a detailed knowledge of the propellant gas properties as they leave the gun and interact with the surrounding atmosphere. Since the ultimate goal is to decrease (or completely eliminate) the flash, a thorough understanding of the phenomena is essential if this is to be accomplished. The final problem which is being experienced in the field is the muzzle blast, or overpressure, which has been observed in both howitzers and 30mm cannon mounted on helicopters. The high pressures created by the blast have an adverse effect on both the gun crews and the surrounding structures. The structural problem is particularly acute when the gun is mounted on a critical structure such as a helicopter (or other aircraft). The solution to this problem is similar to that of the muzzle flash in that any attempt to decrease

the overpressure is completely dependent on having an accurate description of the propellant gas properties as they emerge from the gun barrel.

The measurement of the gas properties has, in the past, been limited to internal pressures and barrel surface temperatures. From these, one can infer the gas temperature by making several assumptions regarding the interior ballistics behavior. These techniques, due to their inherent limitations, do not provide the required information which is necessary for an accurate modeling of the propellant behavior. Optical methods such as photography, schlieren, and shadowgraphs provide useful information, however, it is mostly of a qualitative nature. Other diagnostic techniques such as emission absorption spectroscopy and two color pyrometry can provide quantitative data, but it is generally of an integrated nature rather than a pointwise measurement. A diagnostic method which is pointwise, remote, simultaneous and instantaneous, and can provide most of the necessary information described above is the spontaneous laser based Raman scattering method. As is well known, the spontaneous Raman scattering technique (Ref. 1-17) is capable of providing accurate information on concentration of species, gas temperature, and with special acquisition and processing methods, also fluctuation, correlation and cross correlation parameters.

The present investigation has been conducted with the aim of determining the applicability of the laser based Raman technique to the diagnostics of the flow field at the muzzle of a 20mm gun following the passage of the projectile. This has application to both the muzzle flash and the muzzle blast problems. A subsequent

study could be performed to obtain measurements within the gun barrel; this would be applicable to the barrel erosion problem.

II. The Raman Effect

The Raman effect is the phenomenon of light scattering from a material medium, whereby the light undergoes a wavelength change and the scattering molecules undergo an energy change in the scattering process. The Raman scattered light has no phase relationship with the incident radiation. Based on quantum theoretical considerations, the incident photons collide elastically or inelastically with the molecules to give Rayleigh and Raman lines respectively, with the inelastic process much less probable than the elastic. The process of light scattering can be visualized, as the process of absorption of an incident photon of energy E by a molecule of a given initial state, raising the molecule to a virtual state, from which it immediately returns to a final stationary state emitting a photon of energy equal to the difference in energy between the two stationary states and incident energy E. This is seen graphically in the schematic diagram of Fig. 1, where vibrational and rotational transitions are indicated corresponding to the appropriate vibrational and rotational selection rules which are $\Delta J = 0, \pm 2$ and $\Delta V = \pm 1$. Since the anti-Stokes lines must originate in molecules of higher energy level, which are less abundant at normal temperatures, the anti-Stokes lines would be expected to be much weaker than the Stokes lines. This qualitative description of the Raman effect is obviously very superficial. For a more rigorous and complete discussion of this effect one should consult the cited references.

An inspection of Fig. 1 reveals that the impingement of a photon on a molecule, if Raman active, may result in the excitation of vibrational as well as rotational transitions. Fig. 2 presents an

approximate Raman and Rayleigh scattering response from air illuminated by a Ruby laser. It is evident that the Rayleigh as well as the vibrational spectra have closely associated rotational wings. Since, for our purposes, the vibrational scattering is of direct interest, it is worthwhile to examine the vibrational Raman response. It consists essentially of three branches: (1) the intense Q-branch for which $\Delta J = 0$, (2) the much weaker O-branch for which $\Delta J = 2$, and (3) the S-branch for which $\Delta J = +2$ of approximately the same intensity as the O-branch. The O and S branches are much weaker than the Q-branch and represent only about 1% of the intensity of the Q-branch. They are therefore of minor importance as far as the present applications to fluids are concerned. If a highly dispersive instrument is used, the Q-branch can be resolved into components corresponding to the energy levels characterized by the quantum numbers V = 1,2,3, etc. These of course will appear at elevated temperatures, and may therefore be used to determine the fluid temperature, cf. Fig. 3. Since the orientation of the molecules cannot be fixed in a fluid, the scattering will correspond to an average overall molecular orientation, and the vibrational Raman scattered intensity as derived using the Placzek polarizability theory may be expressed as

$$I_{S,A} = CNI_o \frac{(\nu_o \pm \nu)^4 f(\alpha', \gamma')}{(1-\exp\left[\frac{hc\nu}{kT}\right])}$$

From the relative intensity of the Stokes and anti-Stokes lines, taking account of the Boltzmann factor, the temperature is given by

$$T = \frac{hc\nu}{k} \left[\ell n \frac{I_s}{I_A} + 4\ell n \left(\frac{\nu_o+\nu}{\nu_o-\nu}\right)\right]^{-1}$$

It should be noted that the scattered intensity is proportional to the fourth power of the frequency and to the incident intensity and, of course, to the number density of a given species. It is well-known that the pure rotational Raman spectra appearing near the exciting radiation frequency can be quite intense. However the very small wavelength separation of the lines, particularly in a mixture of gases, makes the pure rotational spectra very difficult to use for diagnostic purposes as defined here in spite of its stronger signals. The weakness of the Raman scattering technique is its low scattering cross-section. Consequently, the signal obtainable is a major factor in determining the applicability of the technique to a given problem. The number of photoelectrons contributing to the signal may be written

$$n_s = E_o N \sigma \ell \Omega \eta_o \eta_g E_p^{-1}$$

where E_p is the energy per photon, η_o is the optical efficiency of the collecting optics, and η_g is the quantum efficiency of the photocathode. The last equation may also be written in terms of an output voltage from a photomultiplier tube across a load R, with a gain G and laser pulse duration t,

$$V_5 = E_o N \sigma \ell \cdot \Omega \eta_o \eta_g \cdot G \cdot eR \cdot (E_p \cdot t)^{-1}$$

where e is the electron charge in coulombs and V_s the signal voltage. The last two equations permit the evaluation of the achievable voltage signal or photon-count in a given situation, if not exactly, at least to a first reasonable approximation. The laser pulse in the above approximation is assumed to have a rectangular shape whereas in actuality the laser pulse generally has a Gaussian

distribution in intensity. The voltage signal or photon count must exceed the signals due to background noise or other disturbing signals, if the measurement is to be useful.

At this point it is clear that, in principle at least, instantaneous and simultaneous data for the determination of species concentration and temperature can formally be obtained. The former because the Raman transition takes place in a time of the order of fractions of picoseconds for most Raman active molecules, if illuminated by light in the visible range; and the second because one may record the Stokes and anti-Stokes intensity at the same time, the number of data points only depending on the number of receiving channels one has available. The vibrational Raman system, which permits clear identification of species involved, is generally used. An obvious difficulty in performing Raman intensity measurements is the extremely small equivalent Raman scattering cross-section. Typically, this cross-section may vary between $10^{-29}cm^2$ and $10^{-31}cm^2$, depending on the molecule under investigation and the frequency of the primary light. Since the frequency dependence is of overriding importance here (fourth power), and is essentially the only parameter which is at the disposal of the experimentalist, one would tend to automatically choose the laser operating at the highest frequency. While this choice might be desirable in one respect, other aspects of this choice might be less favorable as will be discussed later.

The line separation of the resulting Raman spectra is greater for longer wavelength lasers than shorter wavelength sources of primary radiation. This feature may become important in cases where several species are involved and their measurement and resolu-

tion are desired, in particular when narrow bandpass filters are contemplated. Figures 4 and 5 illustrate this problem very clearly, both in terms of concentration measurements of a mixture of gases and the preference of using the ratio of the vibrational Stokes to anti-Stokes intensity for the determination of temperature, as opposed to the rotational spectra. It should also be pointed out that the use of a nitrogen laser at the conventional energy (1mj) levels available, requires the utilization of photon counting techniques and generally mean values of the measured variables are obtained, while with a Ruby laser, due to its much higher energy (4 joules) per pulse, single pulse operation is possible and therefore instantaneous values can be obtained. The latter is also true for a doubled neodymium yag laser operating at 5320Å available at a repetition rate of 10pps at energy levels in excess of 0.5 joules.

In addition to these pulsed lasers, C-W lasers are being utilized to perform Raman measurements. In particular the argon ion laser operated at 5145Å or 4880Å is very useful in steady state systems where mean concentration and temperature are desired. C-W lasers would, of course, be ideal for time resolved Raman measurements of fluctuating flow fields and combustion systems. However, the available commercial lasers are of insufficient power to provide useful data concerning fluctuating systems.

It is therefore apparent from the above that spontaneous laser Raman scattering has all the desired features of an ideal probe. There are, however, problems associated with this diagnostic method. In discussing the feasibility of diagnostics by means of monitoring the intensity of radiation, and particularly scattered radiation re-

sulting from the Raman effect, one must consider the background radiation which may interfere with the desired signal and render it useless. There are a number of sources which may contribute to the undesired background radiation. In order of significance they are: Rayleigh scattering, scattering of the incident beam by viewing port windows, walls and large particles in the flow, Mie scattering, gas particle and surface fluorescence, ambient light, detector dark current, electrical noise, and detector shot noise.

The first two, being of the same frequency as the incident beam and thus spectrally separated from the desired signal, can be filtered out using proper interference filters or spectrographs used for the selection of the desired signals. The fluorescence problem can be a very serious problem. Careful selection of the materials and surface coatings may eliminate this problem. In some cases by proper choice of the primary laser this problem can be avoided. In this respect, the use of a Ruby laser has not caused any significant fluorescent problem in this laboratory. The detector dark current and electrical noise can generally be handled by using photomultiplier coolers, which serve a dual purpose of decreasing the dark current and shielding the photomultiplier from electrical interferences. As far as the shot noise is concerned, this problem must be dealt with at the data processing level.

In general the larger the signal-to-noise ratio the better the system. As has been pointed out,[14] a very convenient parameter to assess the capability of a system is the "feasibility index". This index was defined as $\chi = NL\sigma_0\Omega e$ where N is the num-

ber density of the scatterers per cm^3, L is the length of the sample in the direction of the laser beam, σ_0 reference cross-section, and Ω and e the solid angle and optical efficiency, respectively. The minimum feasibility index for a 1 joule Ruby laser in a single pulse operation is approximately 10^{-15}. Thus, for a situation where this index is below 10^{-15} a 1 joule single pulse laser would not provide the desired information. An increase in the laser energy or any of the other factors may be necessary. There is, however, a limit on the laser energy one may apply. The laser energy density should be below the breakdown threshold which for Ruby and air appears to be around $10^{10} W/cm^2$.

The choice of the proper method of spectral analysis can be very important. There are basically three methods available: the standard monochromators, interference filters, and Fabry-Perot interferometers. Each has a range of applicability and its positive as well as negative features. The interested reader may consult standard texts or some of the following references.[10],[15],[18]

The detection of the scattered photons of interest is best accomplished by photomultipliers. They are the most sensitive low level light detectors available at present, applicable in the wavelength range from u.v. to near infrared or from about 3-10 thousand Angström wave length. The output of the photomultiplier may be used in one of several ways: (i) as an input to a d.c. amplifier, (ii) as an input to a photon counter, (iii) as an input to a phase sensitive detector, or as a combination or modification of the above basic schemes.

In general photon counting is more accurate than a direct reading of the photomultiplier current. The reasons are: (i) the d.c.

level caused by leakage currents of photomultiplier tubes cannot be detected by photon counters, (ii) the statistically varying heights of the detector output pulses are replaced by standard height pulses, (iii) the photon counting rate can be made insensitive to power supply voltage fluctuations with proper care. However, at high photon count rates, photon counting may present some difficulties particularly if the detection rate exceeds about 10^7 counts/sec.

Recently a new detection system has been introduced. It offers a number of advantages over photomultiplier tubes. It is supposed to be capable of providing simultaneous measurements of the Raman scattering signals of a multiplicity of species at many spatial points, during a single laser pulse. It would therefore be capable, in conjunction with proper computational facilities, of providing in addition to concentration and temperature, data necessary for the determination of spacial correlation functions. Among the commercial units on the market the OMA2 system appears to be the best both in terms of reliability and operational versatility. Although some of the sensitivity claims for the several detection systems are somewhat overstated relative to the commercially available photomultiplier tubes, it still represents a major advance in the laser scattering diagnostic technology.

III. Experimental Facility

Since the primary aim of this study was to determine the feasibility of utilizing the spontaneous Raman effect for the diagnostics of the muzzle flow field, a 20mm gun was set up for the experiments. Although the actual problems occur in much larger caliber guns, it was felt that a 20mm gun was the largest that could be used in a laboratory-type environment. Moreover, the basic flow phenomena in terms of the muzzle flash, overpressure, etc. should be quite similar even in a relatively small bore such as a 20mm gun.

The gun was obtained from BRL and was mounted on a heavy duty steel support embedded in a concrete base. The laser, the firing mechanism, and the data acquisition equipment presently consisting mainly of high speed oscilloscopes, power supplies and connectors were mounted within a concrete walled control room; an access hole for the laser beam was drilled through the wall to the test chamber. A projectile catcher constructed by the BRL and filled with sand was installed approximately 10 feet from the muzzle exit. This provided adequate room for the installation of adjustable telescopes and photomultiplier tubes for the acquisition of the Raman scattered radiation, and also for the installation of a shadowgraph system.

Figure 6 provides a schematic diagram of the experimental configuration. As can be seen, the gun has been equipped with four kistler pressure transducers: one near the breach, the second 9-5/16" from the end of the muzzle and, the remaining two transducers 1.5" apart, as seen in Figure 7, in the end "addition" to the muzzle. Three electrostatic probes have also been mounted

near the muzzle which, in conjunction with a start-stop time interval counter, can indicate the projectile exit velocity. This velocity can also be obtained using the two muzzle pressure transducers.

The shadowgraph system consisting of a 4 ft focal length 8" diameter parabolic mirror, a triggerable spark located at the focal point and synchronized with the projectile exit position, a projection screen, and a photographic apparatus permits the acquisition of photographs which provide qualitative information on the flow field observables.

Before describing the laser Raman system, it must be mentioned that after reviewing some of the literature and taking note of some of the difficulties experienced by other investigators who were attempting to use a Ruby laser for the diagnostics of the muzzle exit flow field, it was decided to investigate the radiation spectrum of the projectile plume. For that purpose two types of multichannel spectrum analyzers available at the time in our laboratory were utilized. It was found that the emission spectrum of the flow field behind the projectile was in the near infrared region, overlapping the Raman lines produced by a ruby laser. The emission spectrum was observed to extend over the range from approximately 6000Å to 9000Å. The exact emission lines have not been determined due to some difficulties in calibration of the multichannel analyzers. However, it became obvious that due to the intensity and location of the emission spectrum it would not be prudent to rely exclusively on the spontaneous Raman scattering spectrum excited by a Ruby laser. This spectrum would fall exactly within the emission spectrum of the hot propellant gases following

the projectile.

It was therefore decided to utilize a doubler on the Ruby laser; this would shift the Raman spectrum into the region of 3000Å to 4000Å which is well outside the emission spectrum of the propellant gases. The conversion efficiency of the doubler is approximately 20%; with an initial laser pulse energy of 3 joules at 6943Å, the expected output of the doubler is approximately 600mj. As indicated previously, the Raman scattering intensity is proportional to the incident laser energy and to the fourth power of the incident frequency. It is therefore evident that as far as the scattered intensity is concerned, in spite of an 80% loss in the incident power there will be a gain of about 300% due to the increased frequency. Difficulties in terms of spectral line density as indicated above must be dealt with by using very narrow bandpass filters or very selective spectrometers. Since most of the original ruby laser energy is still available it was decided to utilize it in its original form, as seen in Figure 6. After separating the doubled laser light using a dichroic mirror, the remaining 6943Å laser radiation was directed by a mirror and refocussed at the same point as the 3472Å doubler output. It is thus possible to utilize simultaneously two laser frequencies for the acquistion of the pertinent data. Due to the availability of only two sets of photomultiplier tubes suitable for the two given spectral ranges, and the desirability of measuring the temperature, it was decided to concentrate on the measurement of the Stokes and anti-Stokes intensities of nitrogen. To this end each photomultiplier tube was equipped with its own telescope, narrow bandpass filters, and band stop filters. Two photo-

multipliers were of RCA type 8853 and two of EMI type 9813QA. The former were used for the Stokes and anti-Stokes resulting from the 6943Å incident radiation, the latter from the 3473Å wavelength. The Stokes and anti-Stokes filters for the nitrogen molecules corresponding to the 6943Å incident radiation were centered at 8283Å and 5976Å respectively, while the bandpass filters for Stokes and anti-Stokes radiation corresponding to the 3472Å incident radiation were centered at 3776Å and at 3211Å. The mounting planes for the two sets of tubes were 90° to each other to correspond to the respective planes of polarization of the two laser beams.

The tests were initiated by firing the gun using the electrical remote firing device. In order to synchronize the transit of the projectile and the firing of the laser, a pressure transducer was utilized to trigger the laser, through an intermediary time delay and triggering generator system. A second time delay system was used to place the laser pulse at an exact, predetermined position behind the projectile. This delay was adjustable to fractions of a microsecond. The sweeps of the recording oscilloscopes were initiated by the laser itself through the photodiode. The data could be directed either towards the recording oscilloscopes or the data acquisition and processing system, as indicated in Figure 6.

IV. Discussion of Results

A test is initiated by firing the gun from a remote electrical switch. The laser is triggered by the output of transducer No. 3 (Fig. 7) through a series of delayed generators which also initiate the oscilloscopes used to record the pressure of transducers No. 1 and No. 2.

The photodiode indicated in Figure 6 is used to monitor the laser energy as well as to initiate the sweep of the high speed recording oscilloscopes. Pressure transducer No. 3 also initiates the triggering of the spark system for the shadowgraph.

Figure 8 shows two photographs of three oscilloscope traces each. The upper trace in each of the photographs indicates the time of the laser firing. The lower two traces represent the pressures of transducers No. 2 and No. 1 respectively. The two photographs represent two separate firings of the gun. From the traces, the maximum pressures are 1200psi and 1000psi for the upper and lower traces respectively, corresponding to pressure transducers No. 2 and No. 1. Figure 9 represents the Stokes and anti-Stokes intensity of N_2 behind the projectiles. While the signals appear to be clean and intense, the subsequent firings indicated the same ratio of Stokes to anti-Stokes as well as the same amplitude, even though the point of measurement relative to the passing of the projectile was changed from test to test. It should be mentioned here that the position of measurement could be adjusted by an appropriate time delay selection of the laser firing with respect to the projectile passing transducer number 3. This is illustrated in Appendix A. Since the muzzle temperature (and hence the ratio of Stokes to anti-Stokes intensity) should vary with time,

or with projectile distance from the muzzle, the lack of dependence of the measured data on the projectile position casts some doubt on the veracity of these measurements. It is believed that some extraneous radiation may have produced these anomalous data. In order to find the source of this radiation and the cause of it, several additional tests have been conducted. These tests attempted to confirm or disprove several assumptions made as to the origin of this radiation.

The first assumption was that this radiation was associated with some kind of leakage of incident laser light into the receiving tubes. To test this assumption the laser was fired into the atmosphere without the gun being fired; the firing of the laser indicates a Stokes line corresponding to the nitrogen content of the atmosphere. The anti-Stokes line indicates a negligible signal since the air is at ambient temperature. Figure 10 shows these results which elminate the possibility of any leakage of incident radiation to the photomultiplier tubes.

The second possibility was that there might still be some radiation from the hot gases behind the projectile in the spectral region corresponding to the doubled ruby (3000-4000Å) in spite of the results obtained from the multichannel spectrum analyzers as indicated previously. To examine this assumption, the gun was fired, however the laser was not fired. It is evident from examination of Figure 11 that there is no resulting signal. This confirms the previous findings that in this spectral region the emissivity of the propellant gases is negligible.

In order to further check out the operation of the system, the laser was fired into an air-methane flame placed in front of the

muzzle and the Stokes and anti-Stokes signals were recorded. The temperature of the flame was found from these signals and it agrees with the temperature as measured with a very thin Platinum-Platinum 10% Rhodium thermocouple. The Stokes and anti-Stokes signals were those of nitrogen using exactly the same focussing, filtering and recording system as shown in Figure 9.

The third possible explanation was that the recorded signal was a result of laser induced fluorescence. While this may be possible, it is believed that the overwhelming contribution to the undesired signal is Mie scattering. This type of scattering, besides being by far the strongest, is also directional. In order to verify this supposition the filters from one telescope and photomultiplier were changed to the other. This caused the scattering direction to change, producing a large change in the signals. This being the case, it is believed that this type of scattering (being of the same wavelength as the incident beam) can be eliminated either by increased filtering or by introducing very selective monochromators. In either case it is believed that temperature and specie concentration in the flow field behind the projectile can be obtained by proper modification of the experimental set up.

It is our desire to perform these measurements by the use of narrow bandpass and band elimination filters. The filter method permits one to use a large number of data receiving systems simultaneously whereas the utilization of monochromators is less economical and more restrictive because of their size.

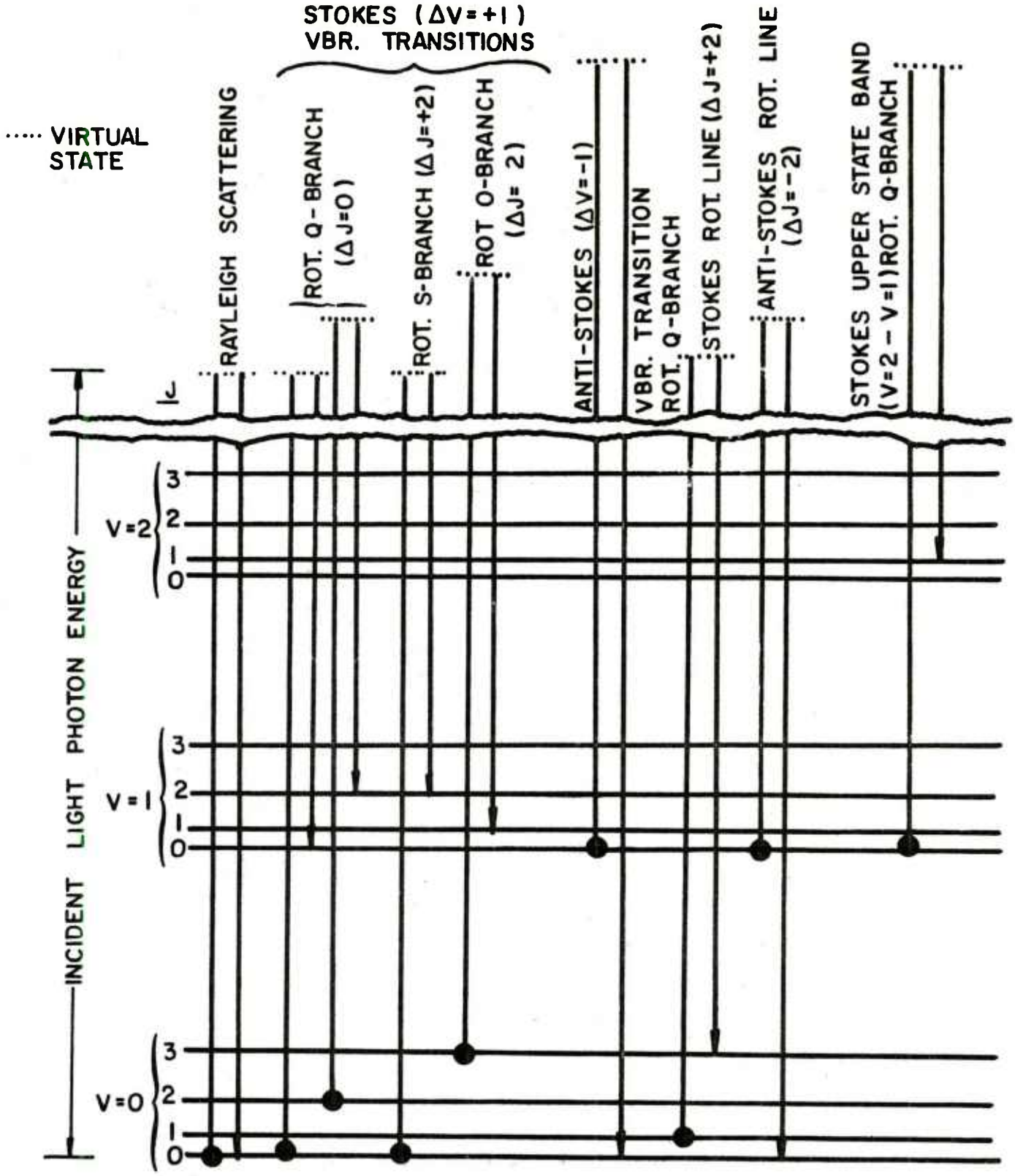

FIG. 1 SCHEMATIC DIAGRAM OF MOLECULAR TRANSITIONS

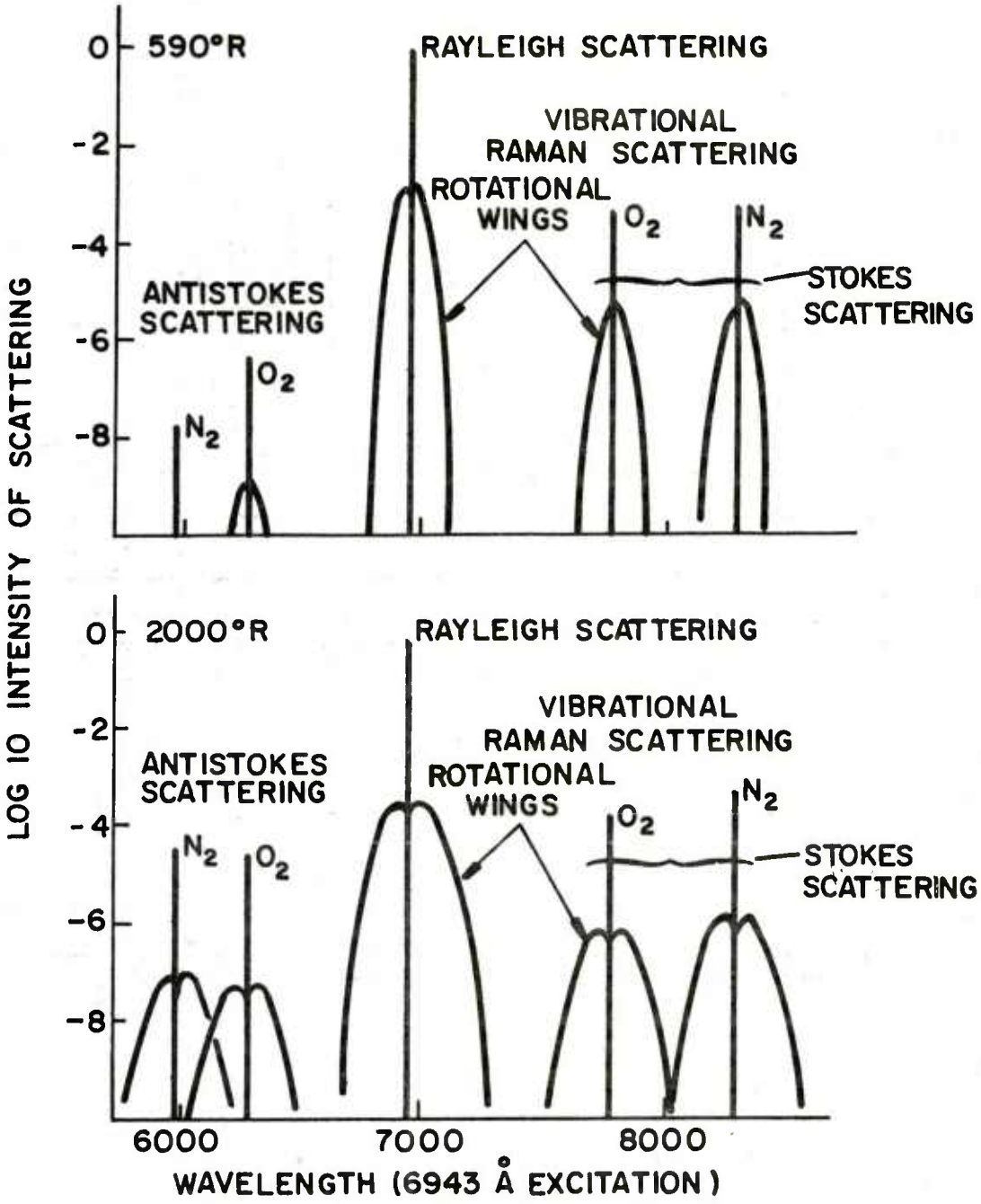

FIG. 2 RAMAN AND RAYLEIGH SCATTERING FROM AIR

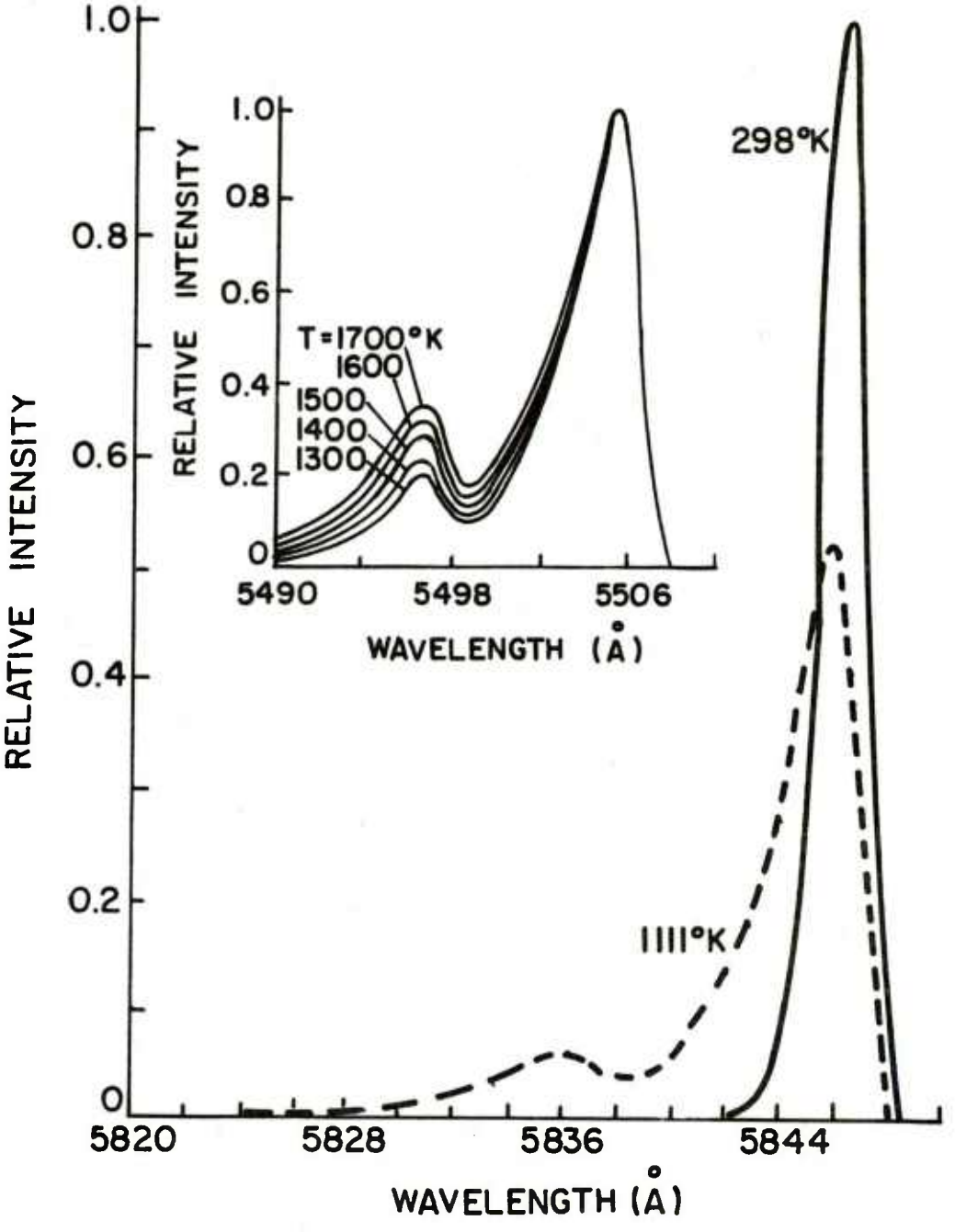

FIG. 3 THE RESOLVED Q-BRANCH

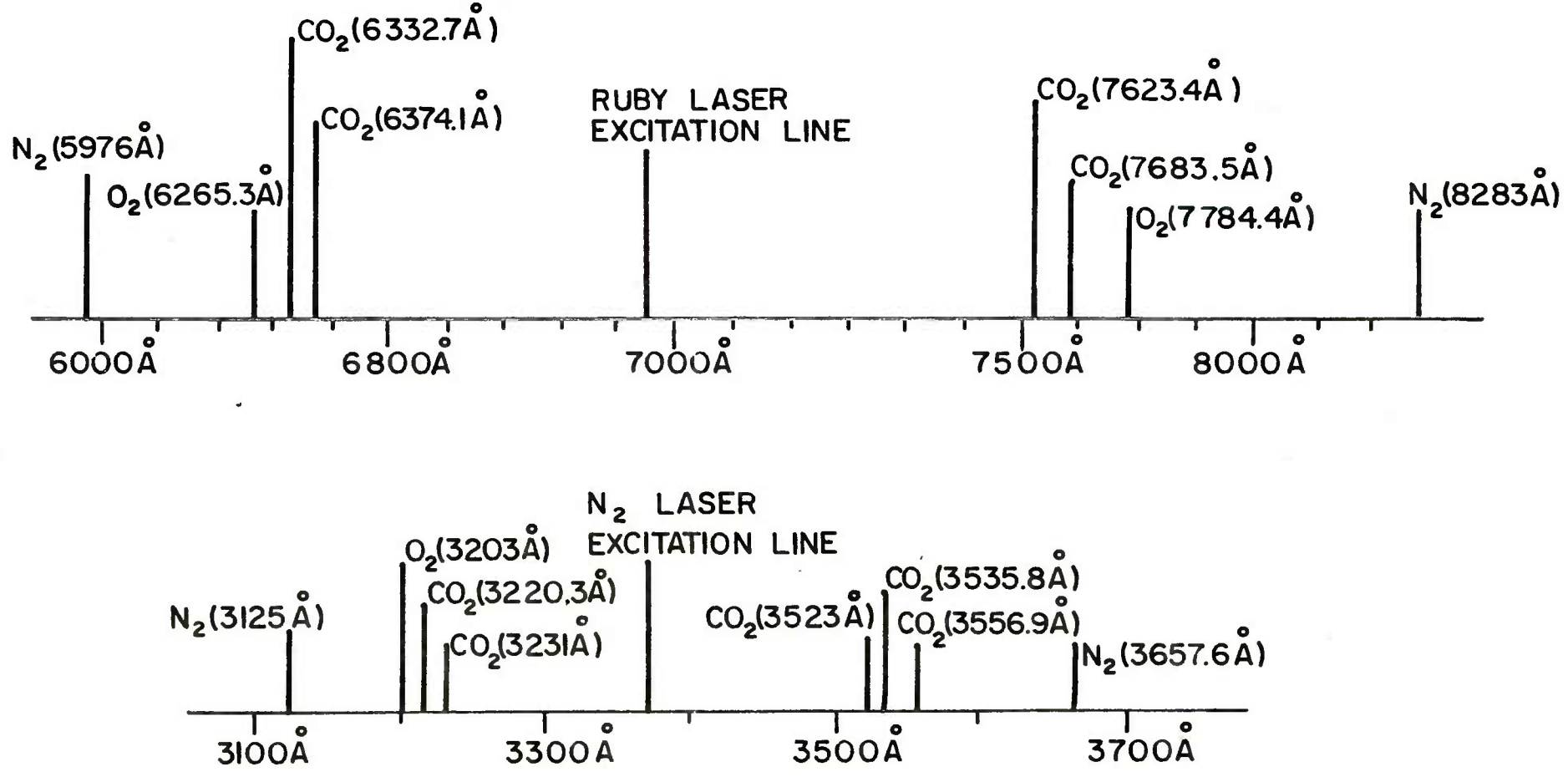

FIG. 4 VIBRATIONAL LINE DENSITY AS A FUNCTION OF 3 GASES

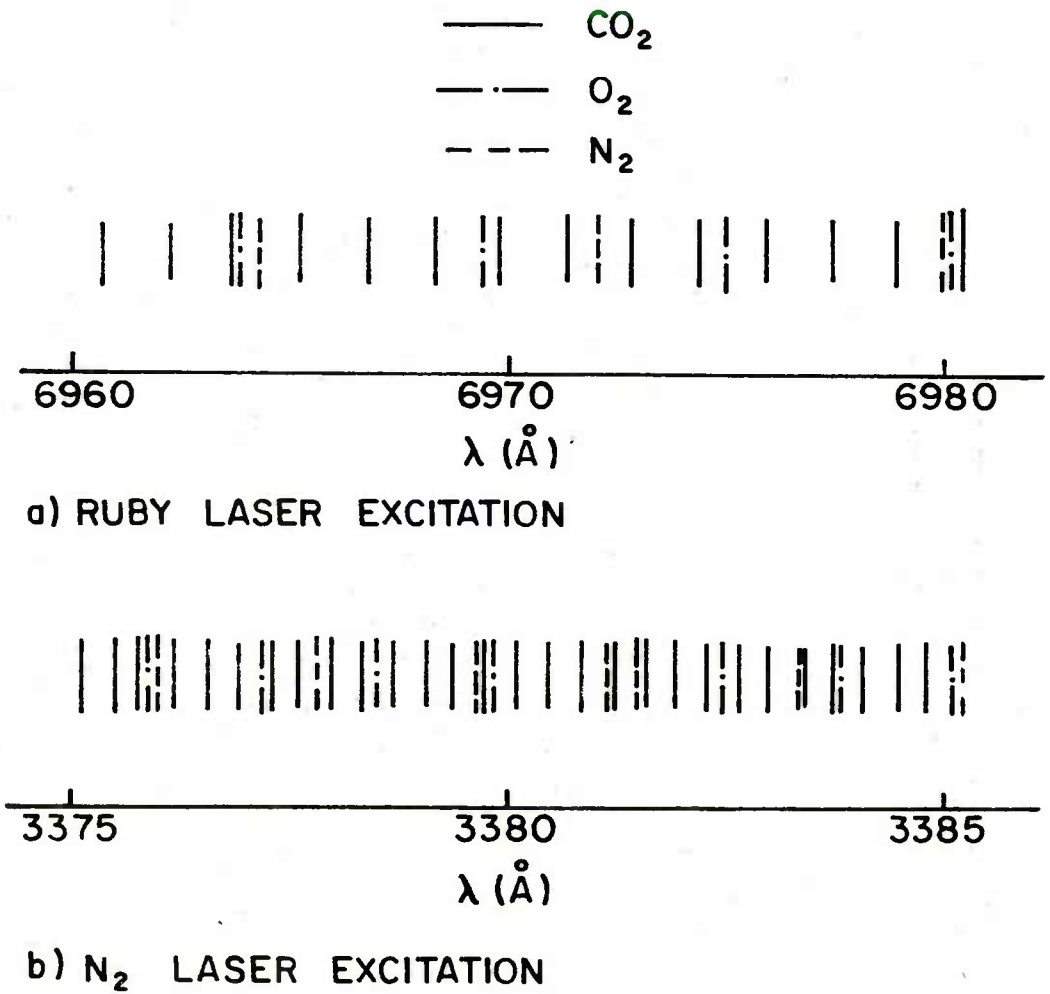

FIG. 5 ROTATIONAL LINE DENSITY OF A MIXTURE OF 3 GASES

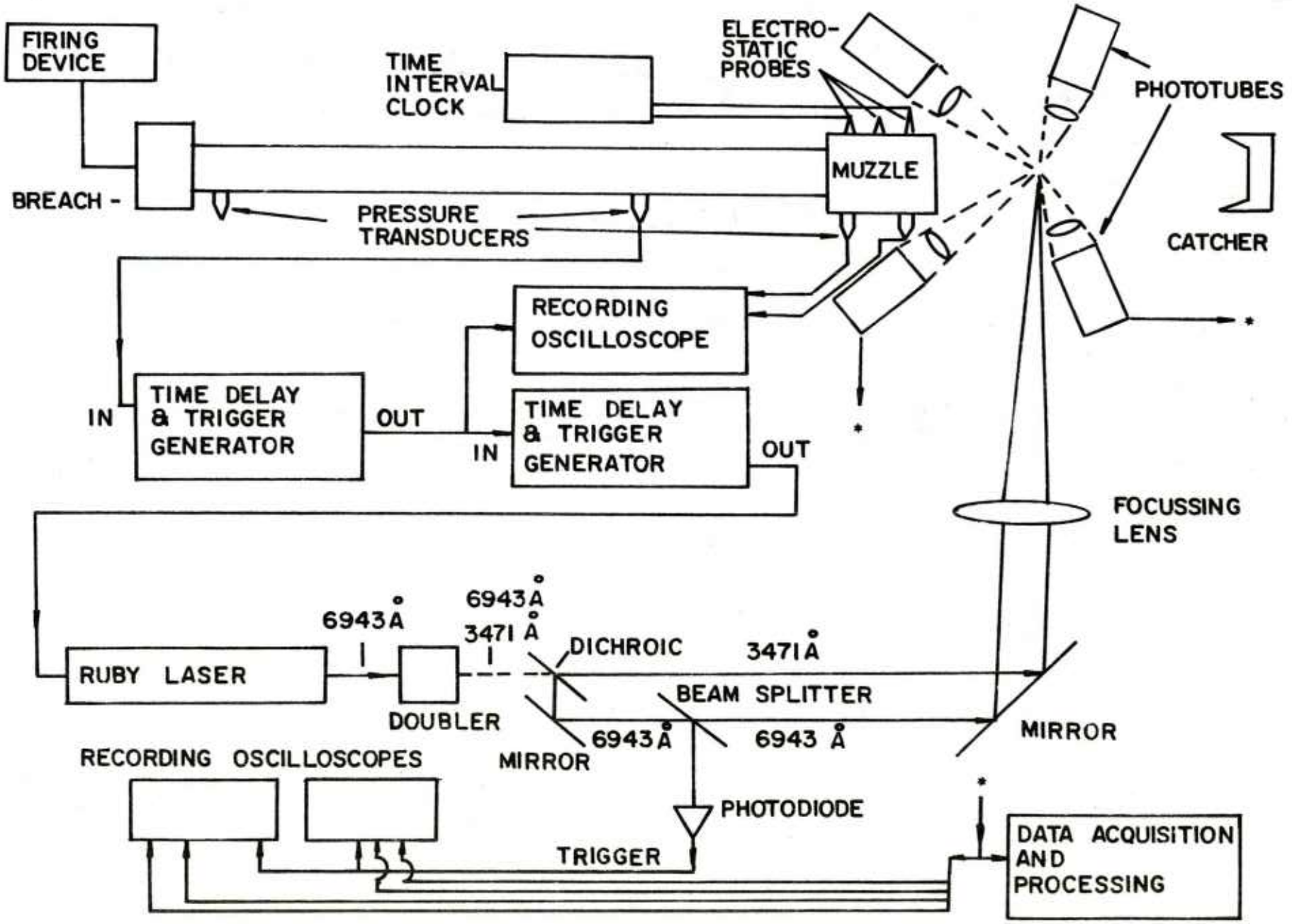

FIG. 6 SCHEMATIC DIAGRAM OF EXPERIMENTAL CONFIGURATION

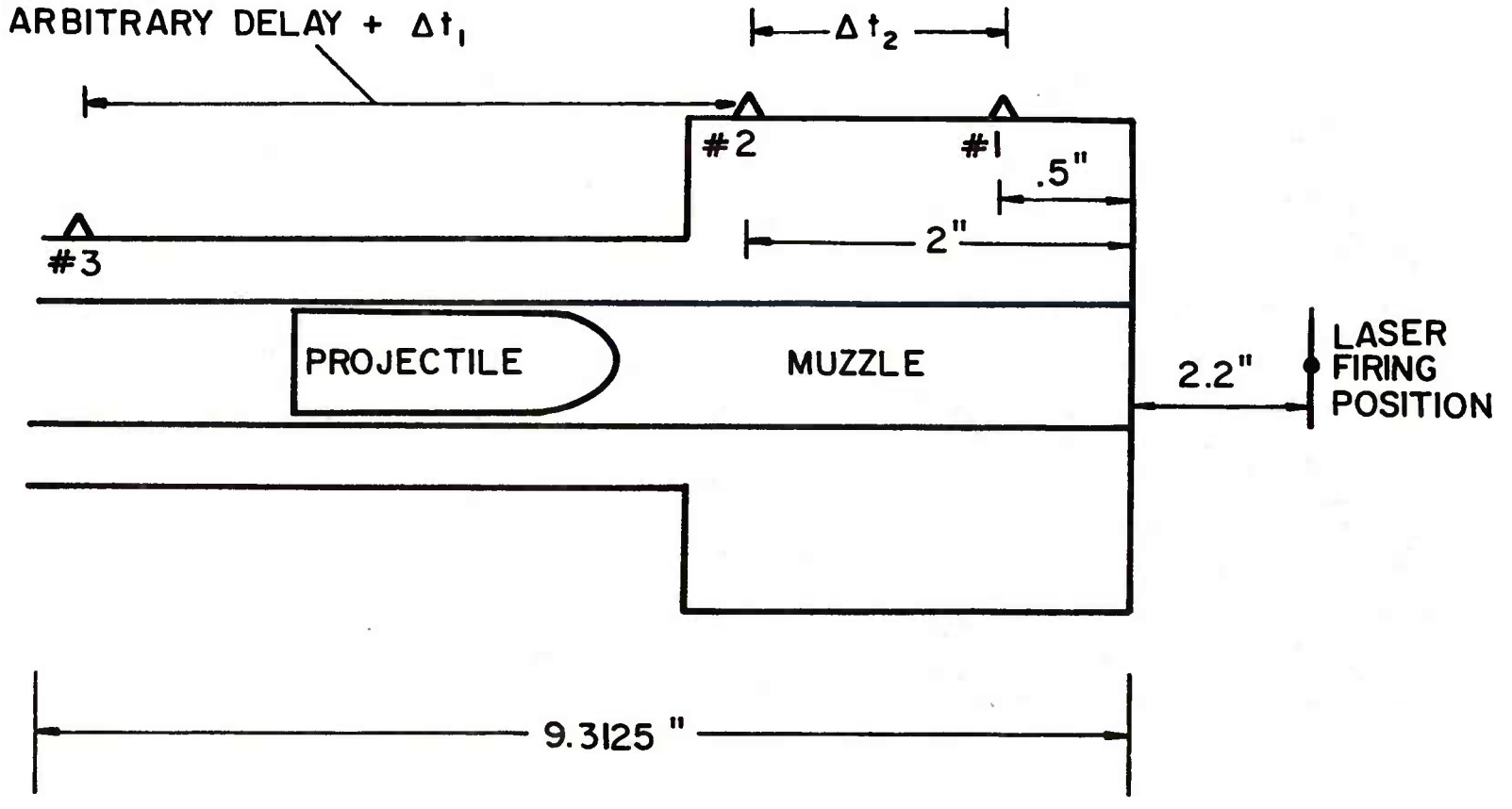

FIG. 7 GUN BARREL PRESSURE INSTRUMENTATION

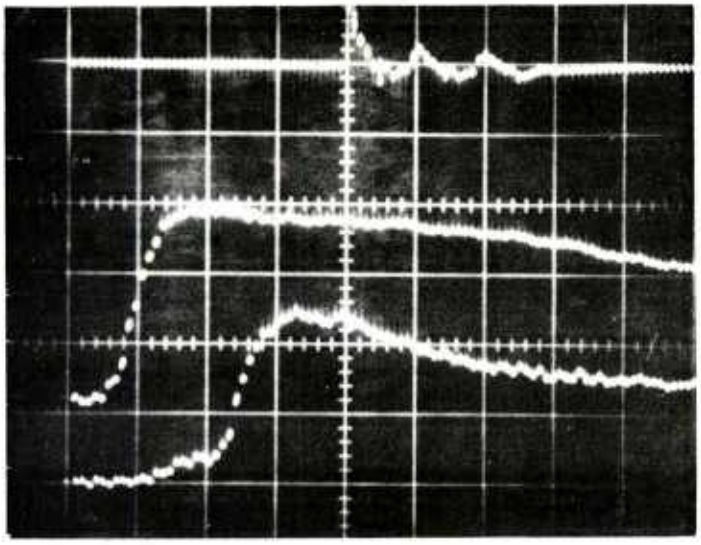

TEST # 210

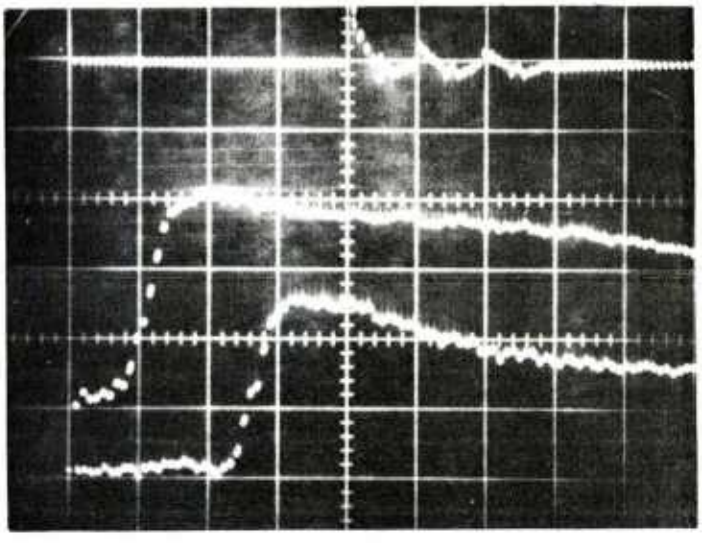

TEST # 211

FIG. 8 TEST DATA

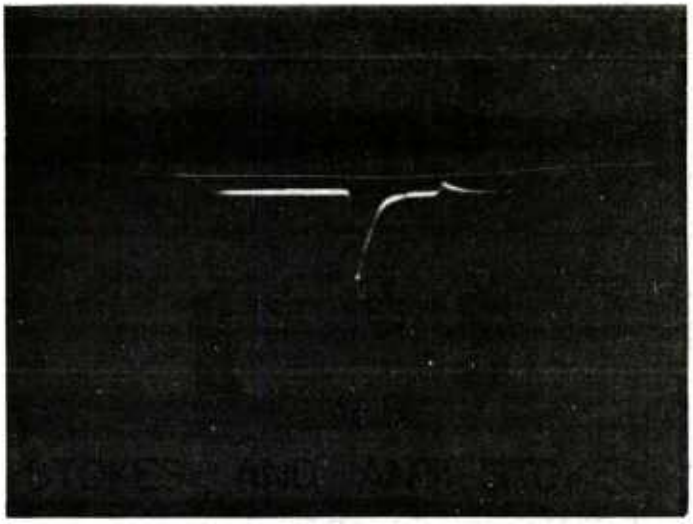

ANTI-STOKES

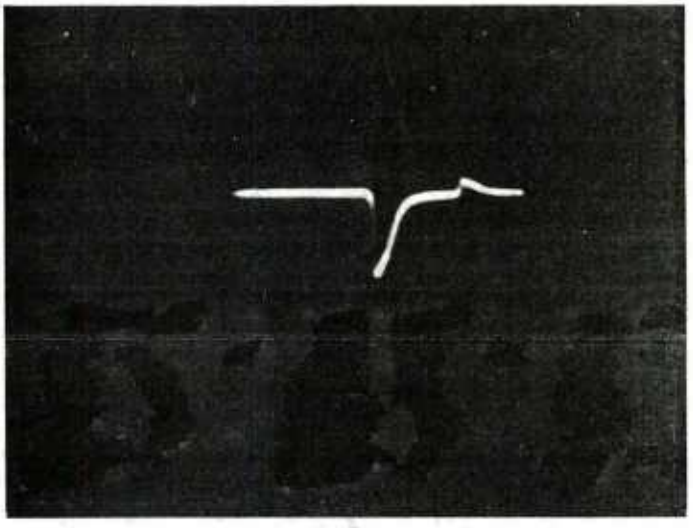

STOKES

FIG. 9 STOKES AND ANTI-STOKES DATA FOR A TYPICAL TEST

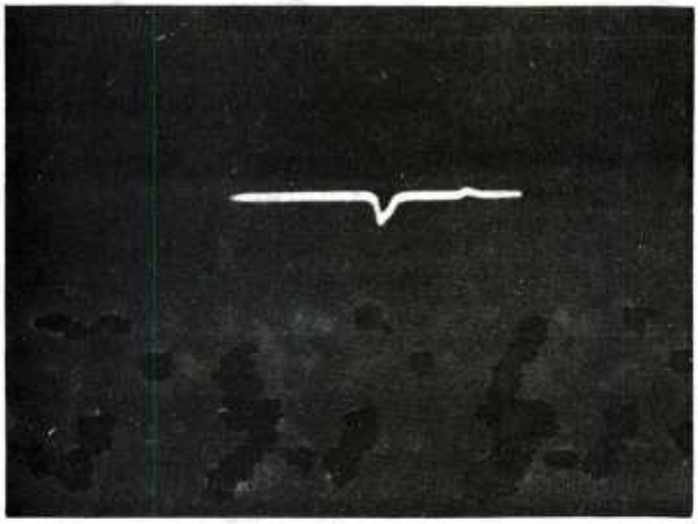

STOKES

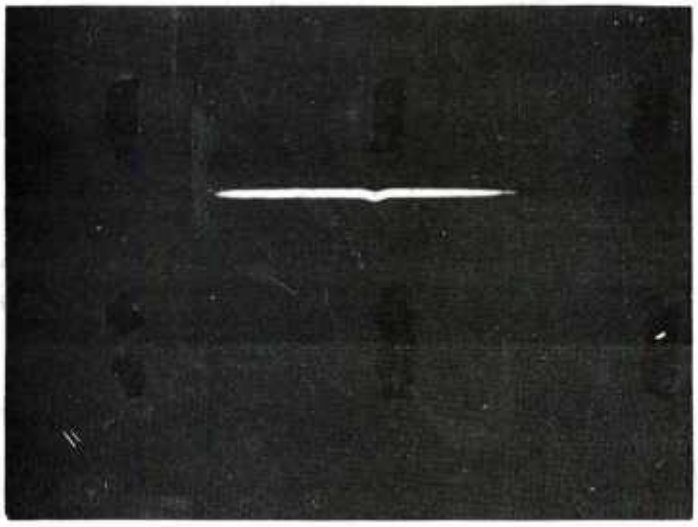

ANTI-STOKES

FIG. 10 STOKES AND ANTI-STOKES DATA FOR ATMOSPHERIC NITROGEN

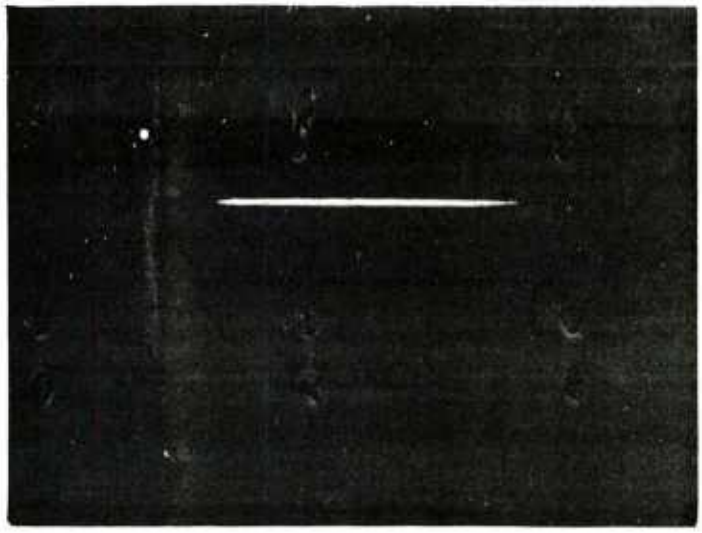

ANTI-STOKES

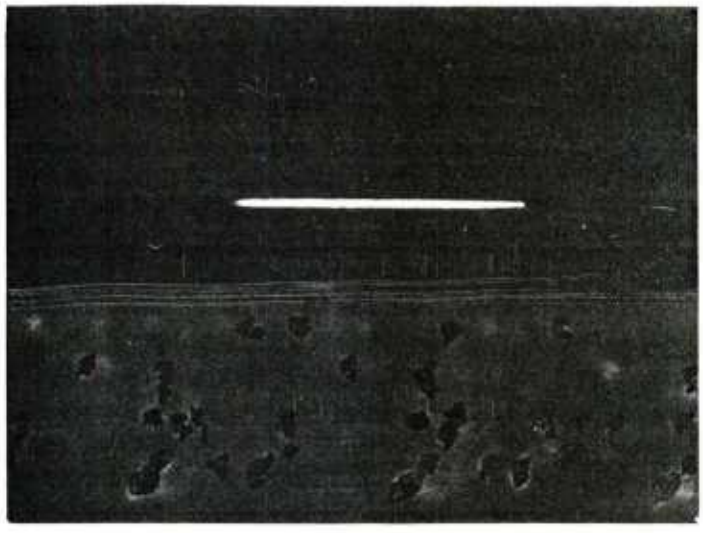

STOKES

FIG. 11 STOKES AND ANTI-STOKES DATA FROM MUZZLE FLASH

References

1. G. Placzek: Handb. Radial. Akademisebe Verlaqsqesellschaft VI (1939).

2. C.M. Sadowski & Y.E.H. Vanoverschelde, CARDE TN 1764167.

3. F. Robben: Project Squid ONR PU-R1-76 1975.

4. H.C. Van de Hulst: Light Scattering by Small Particles, Wiley N.Y. (1957).

5. G. Herzberg: Spectra of Diatomic Molecules, Van Nostrand, NY 1963.

6. H.A. Szymanski ed.: Raman Spectroscopy Theory and Practice, Plenum Press 1967.

7. A. Anderson ed.: The Raman Effect, Bekker, NY 1971.

8. B.P. Stoicherff: High Resolution Raman Spectroscopy, Adv. Spectr. I, pp. 91-174, Interscience (1959).

9. M. Lapp, C. Penny eds.: Laser Raman Gas Diagnostics, Plenum Press, NY, London 1974.

10. M. Lapp, C. Penny: Infr. and Raman Spectr., 3, p. 204 (1977).

11. C. Widhopf, S. Lederman: AIAA J., 9, 1971.

12. S. Lederman, M.H. Bloom, J. Bornstein, P.K. KHosla: Int. J. Heat and Mass Transfer, 17, p. 1479 (1974).

13. T. Yoshino, H.J. Bernstein: J. Mol. Spectr., 2, p. 213 (1958).

14. R. Goulard: Quant. Spectrosc. Rad Transfer, 14, p. 969 (1974).

15. S. Lederman: Prob. Energy Comb. Sci., Pergamon Press, 3, pp. 1 (1977).

16. S. Lederman: AIAA Paper No. 76-21 (1976).

17. S. Lederman: AIAA Paper No. 76-26 (1976).

18. A. C. Eckbreth, P.A. Bomczyk, J.F. Verdieck: Appl. Chem. 8, Plenum, (1976).

Appendix A - Calculation of Projectile Position

The laser beam travels normal to the gun axis and crosses it at a location 2.20 inches from the muzzle. The various time delays in the firing system permit the laser to be fired at different times corresponding to various projectile locations after leaving the gun muzzle. The data shown in Fig. 8 correspond to Run No. 210 and will be used to describe the procedure for determination of the projectile location at the instant the laser is fired and the test data obtained.

The sweep initiation of the oscilloscope trace shown in Fig. 8 was delayed 340μs from the time the projectile base passed the No. 3 pressure transducer. The laser trigger was delayed an additional 200μs from this point (note the top trace of the top photo in Fig. 8). A switch delay of an additional 500μs occurs prior to the laser firing. This delay is inherent in the laser design and cannot be altered; it is this delay which precludes firing the laser from one of the transducers close to the muzzle. The total delay between the laser pulse and the projectile passing transducer No. 3 is therefore given by:

$$340 + 200 + 500 = 1040\mu s$$

The measured time of travel of the projectile between transducers No. 3 and No. 1 is found from Fig. 8 to be:

$$340 + 110 = 450\mu s$$

The time elapsed between the projectile passing transducer No. 1 and the laser firing is the difference between the two computed times or:

$$1040 - 450 = 590\mu s$$

The projectile velocity as it leaves the muzzle is computed by measuring the time of travel between transducers No. 1 and No. 2 which are located quite close to the muzzle. For this test, the velocity was found to be 1667fps. As a result, the projectile location at the time of the laser firing is found by:

590μs (1667) = 11.8 inches

Since the laser beam is located 2.2" from the muzzle, the test is seen to occur when the projectile base is 11.3 inches from the muzzle, or, 9.1 inches from the laser diagnostics location.

DISTRIBUTION LIST

No. of Copies	Organization
12	Commander Defense Technical Info Center ATTN: DDC-DDA Cameron Station Alexandria, VA 22314
2	HQDA (DAMA-WSA, MAJ Csoka; DAMA-CSM, LTC Germann) The Pentagon Washington, DC 20310
1	Commander US Army Ballistic Missile Defense Systems Command Huntsville, AL 35804
1	ODCSI, USAREUR & 7A ATTN: AEAGB-PDN (S&E) APO New York 09403
1	Commander US Army Materiel Development and Readiness Command ATTN: DRCDMD-ST 5001 Eisenhower Avenue Alexandria, VA 22333
1	Commander US Army Materiel Development and Readiness Command ATTN: DRCDL 5001 Eisenhower Avenue Alexandria, VA 22333
1	Commander US Army Materiel Development and Readiness Command ATTN: DRCDE-R, Mr. Lockert 5001 Eisenhower Avenue Alexandria, VA 22333
4	Commander US Army Armament Research and Development Command ATTN: DRDAR-LC, Dr. Frasier DRDAR-SCW, Mr. Townsend DRDAR-SG, Dr. T. Hung PM, 30mm Ammo, LTC Logan Dover, NJ 07801
6	Commander US Army Armament Research and Development Command ATTN: DRDAR-TSS (2 cys) DRDAR-LC-F, Mr. A. Loeb DRDAR-SCA, Mr. N. Ford DRDAR-LCW, Mr. M. Salsbury DACPM-CAWS, Mr. Barth Dover, NJ 07801
2	Commander US Army Armament Materiel Readiness Command ATTN: DRSAR-LEP-L, Tech Lib Rock Island, IL 61299
3	Director US Army ARRADCOM Benet Weapons Laboratory ATTN: DRDAR-LCB-TL Dr. G. Carofano Dr. C. Andrade Watervliet, NY 12189
2	Commander US Army Aviation Research and Development Command ATTN: DRDAV-E DRCPM-AAH, Mr. Corgiatt 4300 Goodfellow Boulevard St. Louis, MO 63120
1	Director US Army Air Mobility Research and Development Laboratory Ames Research Center Moffett Field, CA 94035
1	Commander US Army Communications Rsch and Development Command ATTN: DRDCO-PPA-SA Fort Monmouth, NJ 07703
1	Commander US Army Electronics Research and Development Command Technical Support Activity ATTN: DELSD-L Fort Monmouth, NJ 07703

DISTRIBUTION LIST

No. of Copies	Organization
1	Commander US Army Missile Command ATTN: DRSMI-R Redstone Arsenal, AL 35809
1	Commander US Army Missile Command ATTN: DRSMI-RBL Redstone Arsenal, AL 35809
1	Commander US Army Missile Command ATTN: DRSMI-RLH, (Ricks) Redstone Arsenal, AL 35809
1	Commander US Army Missile Command ATTN: DRSMI-RDK Redstone Arsenal, AL 35809
1	Commander US Army Missile Command ATTN: DRSMI-YDL Redstone Arsenal, AL 35809
1	Commander US Army Tank Automotive Research & Development Command ATTN: DRDTA-UL Warren, MI 48090
1	Commander US Army Research Office ATTN: CRD-AA-EH P. O. Box 12211 Research Triangle Park NC 27709
1	Commander US Army Aeromedical Rsch Lab ATTN: SGRD-UAH-AS, Dr. Patterson P. O. Box 577 Fort Rucker, AL 36362
1	Commander US Army Medical Research and Development Command ATTN: SGRD-ZBM-C, LTC Lamothe Fort Detrick, MD 21701
2	Director US Army TRADOC Systems Analysis Activity ATTN: ATAA-SL, Tech Lib ATAA-S White Sands Missile Range NM 88002
3	Commander Naval Air Systems Command ATTN: AIR-604 Washington, DC 20360
3	Commander Naval Surface Weapons Center ATTN: Code 6X Mr. F. H. Maille Dr. J. Yagla Dr. G. Moore Dahlgren, VA 22448
1	Commander Naval Surface Weapons Center ATTN: Code 730, Tech Lib Silver Spring, MD 20910
1	Commander Naval Weapons Center ATTN: Code 553, Tech Lib China Lake, CA 93555
1	Commander Naval Research Laboratory ATTN: Tech Info Div Washington, DC 20375
1	Commander Naval Ordnance Station ATTN: Code FS13A, P. Sewell Indian Head, MD 20640
1	AFRPL/LKCC, C.D. Penn Edwards AFB, CA 93523
2	AFATL (DLDL, Dr. D.C. Daniel, Tech Lib) Eglin AFB, CA 32542

DISTRIBUTION LIST

No. of Copies	Organization
1	AFWL/SUL Kirtland AFB, NM 87117
1	ASD/XRA (Stinfo) Wright-Patterson AFB, OH 45433
1	Director Division of Medicine WRAIR/WRAMC ATTN: SGRD-UWH-D, MAJ Jaeger Washington, DC 20012
1	Director NASA Scientific & Technical Information Facility ATTN: SAK/DL P. O. Box 8757 Baltimore/Washington International Airport, MD 21240
3	Polytechnic Institute of New York ATTN: S. Lederman R. Cresci T. Posillico Route 110 Farmingdale, NY 11735

No. of Copies	Organization
	Aberdeen Proving Ground
	Dir, USAMSAA ATTN: DRXSY-D DRXSY-MP, H. Cohen
	Cdr, USATECOM ATTN: DRSTE-TO-F
	Cdr, USACSL, Bldg. E3516, EA ATTN: DRDAR-CLB-PA
	Dir, USAHEL ATTN: Dr. Weisz Dr. Cummings
	Dir, USAMTD ATTN: Mr. S. Walton

USER EVALUATION OF REPORT

Please take a few minutes to answer the questions below; tear out this sheet, fold as indicated, staple or tape closed, and place in the mail. Your comments will provide us with information for improving future reports.

1. BRL Report Number _____

2. Does this report satisfy a need? (Comment on purpose, related project, or other area of interest for which report will be used.)

_____

_____

_____

3. How, specifically, is the report being used? (Information source, design data or procedure, management procedure, source of ideas, etc.) _____

_____

_____

4. Has the information in this report led to any quantitative savings as far as man-hours/contract dollars saved, operating costs avoided, efficiencies achieved, etc.? If so, please elaborate.

_____

_____

5. General Comments (Indicate what you think should be changed to make this report and future reports of this type more responsive to your needs, more usable, improve readability, etc.) _____

_____

_____

_____

6. If you would like to be contacted by the personnel who prepared this report to raise specific questions or discuss the topic, please fill in the following information.

Name: _____

Telephone Number: _____

Organization Address: _____

_____

_____